Pergamon

Bioorganic & Medicinal Chemistry, Vol. 4, No. 7, pp 1015–1020, 1996
Copyright © 1996 Elsevier Science Ltd
Printed in Great Britain. All rights reserved
PII: S0968-0896(96)00099-5
0968-0896/96 $15.00+0.00

Site-Directed Mutagenesis of Monofunctional Chorismate Mutase Engineered from the *E. coli* P-Protein

Sheng Zhang,[a] Palangpon Kongsaeree,[b] Jon Clardy,[b] David B. Wilson[a] and Bruce Ganem[b,*]
[a]*Section of Biochemistry, Molecular and Cellular Biology and* [b]*Department of Chemistry, Cornell University, Ithaca, NY 14853, U.S.A.*

Abstract—Analysis of the active-site residues of a fully functional chorismate mutase representing the N-terminal 113 amino acids of the *Escherichia coli* P-protein suggests that Lys39 and Gln88 play critical roles in catalyzing the rearrangement of chorismate to prephenate. Five site-directed mutants at these positions have been constructed in which Lys39 was replaced with Arg, Asn, and Gln, and Gln88 was replaced with Arg and Glu. Although the Gln88Arg plasmid failed to produce detectable cross-reacting proteins in *E. coli*, the other four plasmids were expressed, and the mutant proteins purified to homogeneity. Their structures were similar to wild type enzyme, as indicated by circular dichroism spectra, with Lys39Gln showing a small deviation. In accordance with predictions, all mutations result in major loss of catalytic activity at pH 7.8. However, activity of the Gln88Glu mutant at pH 4.5 exceeded wild-type EcCM. Implications for the mechanism of mutase catalysis are discussed. Copyright © 1996 Elsevier Science Ltd

Introduction

The Claisen rearrangement of chorismic acid (**1**) to prephenic acid (**2**) (Scheme 1) represents the first committed step in the biosynthesis of phenylalanine and tyrosine in bacteria, fungi, and higher plants.[1] The rearrangement is catalyzed by the enzyme chorismate mutase, and has attracted much attention from chemists and biochemists, both because it is an unusually facile Claisen rearrangement and because it is the sole example of an enzyme-catalyzed pericyclic reaction.

Chorismate mutase accelerates the conversion of **1** to **2** about two millionfold, yet despite its central role in the aromatic biosynthetic pathway, the enzyme's catalytic mechanism remains poorly understood.[2,3] Recently, X-ray crystallography has been used to obtain detailed structural information on several chorismate mutases as complexes with synthetic mutase inhibitor **3**.[4] These include (1) EcCM,[5] the N-terminal chorismate mutase domain (residues 1–113) engineered from the bifunctional *E. coli* enzyme chorismate mutase-prephenate dehydratase (P-protein), (2) BsCM,[6] the 127 residue, monofunctional chorismate mutase from *Bacillus subtilis*, (3) ScCM,[7] the allosterically regulated chorismate mutase from *Saccharomyces cerevisiae* (no bound inhibitor), and (4) 1F7,[8] a catalytic antibody generated by linking hapten **3** at the C4-hydroxyl group. Comparison of the three-dimensional structures of the natural enzymes was particularly useful in identifying common active-site motifs and in advancing a working mechanistic hypothesis for chorismate mutases.[9] Here we describe the generation and characterization of active-site mutants in EcCM at two key functional residues.

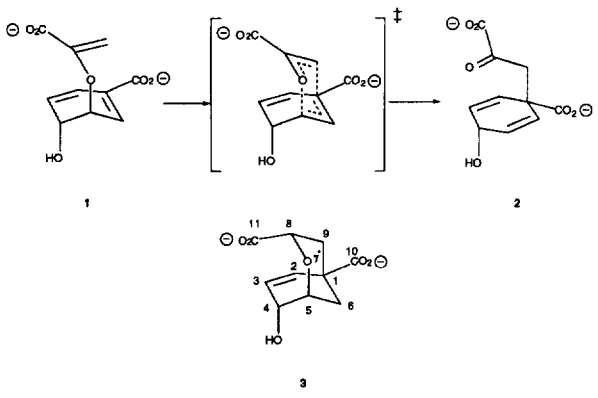

Scheme 1.

Dedicated to Professors Alan Battersby and A. Ian Scott, recipients of the 1995 *Tetrahedron* Prize.

Results and Discussion

From the three-dimensional structure of the EcCM–inhibitor complex (Fig. 1), at least eight amino acids play a role in active-site binding. To identify key catalytic residues, the EcCM, BsCM, and ScCM active sites may be compared by aligning the atoms of bound inhibitor **3**. Two common structural motifs emerge from that analysis.[9] First, a highly charged region is created by the presence of adjacent, protonated residues (Lys39, Arg11′, Arg51 in EcCM; Arg90, Arg7 in BsCM; Arg16, Lys168 in ScCM). This electropositive wall interacts strongly with one flank of chorismate through an elaborate network of bridging hydrogen

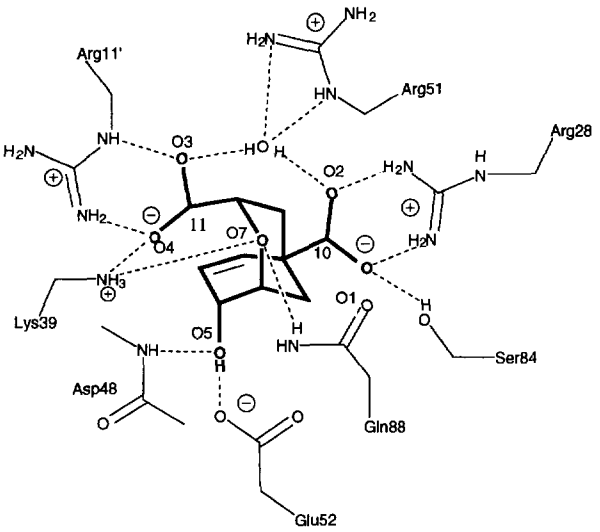

Figure 1. Schematic diagram indicating the hydrogen-bonding and electrostatic interactions of transition state analogue inhibitor **3** with relevant side chains of EcCM, as determined experimentally by X-ray crystallographic analysis.

bonds involving both O7 and the C11 carboxylate of the enol pyruvate. Besides promoting E–S complex formation through electrostatic effects, the positively charged residues in EcCM and BsCM are thought to orient and lock chorismate in the requisite chair conformer for rearrangement.

At the same time, both electron lone pairs on chorismate's vinyl ether oxygen (O7) engage in H-bonding. The resulting two hydrogen bonds in the Claisen transition state are thought to accelerate the rearrangement of chorismate,[10,11] as predicted both from Monte Carlo simulations of aqueous Claisen rearrangements[12] and from experimental studies on synthetic, hydrogen-bonding ureas that catalyze the rearrangement of allyl vinyl ethers.[13] In the case of EcCM, formation of the E–S complex rotates chorismate into position for hydrogen bonding with Lys39 and Gln88. In the ScCM active site, a similar pair of hydrogen bonds is created using Lys168 (which replaces EcCM's Lys39) and Glu246 (which substitutes for EcCM's Gln88). In the case of BsCM, chorismate's enol ether oxygen forms two hydrogen bonds with Arg90. These hydrogen bonds are thought to stabilize the transition state and reduce the activation enthalpy for rearrangement.[9]

Thus, it would appear that the action of Lys39 is central to the proposed mechanism in EcCM, serving both as a cationic residue and H-bond donor. Complementing this residue is Gln88, which provides the second, catalytically important hydrogen bond in EcCM. Both residues were, therefore, judged to be of interest in designing mutagenesis studies.

Mutagenesis and isolation of plasmids

Lysine-39 was replaced with Arg, Asn, and Gln via site-directed mutagenesis using the polymerase chain reaction (PCR) overlapping extension method.[14] The unique restriction sites *Asc* I, *Apo* I, and *Mfe* I created in Lys39Arg, Lys39Asn, and Lys39Gln, respectively, were used to screen for transformants after cloning the PCR products into NK6024 cells. The plasmids were named pSZ27, pSZ28, and pSZ29, respectively. The unique site *Hpa* I was used to screen for Gln88Glu and Gln88Arg transformants. The plasmids pSZ30 and pSZ31 coding for Gln88Glu and Gln88Arg, respectively, were isolated. All plasmids were shown by sequencing to possess only the single expected mutation in their structural gene and promoter region.

Protein expression and purification

All cultures were grown in the same fashion, and mutant proteins were expressed at varying levels. When mutant protein expression was measured by Western blotting, Gln88Arg was not detected in the pSZ31 extract. In order to eliminate the possibility that another mutation occurred upstream of the promoter region for Gln88Arg during the process of PCR that affected expression, the DNA insert from pSZ31 was reinserted into pJS47 from which the wild-type structural gene was deleted. Expression of the plasmid was checked again as above and no expression was detected. These results suggest that the Gln88Arg mutant protein, with its larger side chain and its positive charge, may fold incorrectly and be degraded.

Efficient overexpression of Lys39Arg, Lys39Asn, Lys39Gln, and Gln88Glu was carried out following an earlier protocol[15] to give 20–30% of the soluble protein. Although no large differences were found between the wild-type and mutant enzymes during purification, Gln88Glu, Lys39Asn, and Lys39Gln proteins bound more tightly to the Q-Sepharose column and required elution using a 0–200 mM NaCl gradient (see Experimental section). Since binding of the wild-type and Lys39Arg enzymes to the Q-column was weak, use of 10 mM CAP buffer (pH 10.4) significantly improved the yields.

On an ACA54 gel-filtration column, the Gln88Glu mutant behaved like the wild-type dimer.[5] However, all three K39 mutants eluted earlier, suggesting higher order structures. The yields of the purified enzymes ranged from 6 to 10 mg/L of culture for wild-type EcCM, Gln88Glu, Lys39Gln, and Lys39Arg to 25 mg/L for Lys39Asn. All the purified proteins were analyzed for purity by SDS–PAGE (Fig. 2).

Circular dichroism studies

The secondary structure of each mutant was analyzed using circular dichroism (CD). Spectra of the four mutant proteins were essentially superimposable with that of the wild-type EcCM (Fig. 3), and displayed strong minima at ca. 210 nm and weaker minima at ca. 220 nm, consistent with the known, predominantly α-helical, structure of EcCM.[16] In the case of the Lys39Gln mutant, the observed minima were somewhat

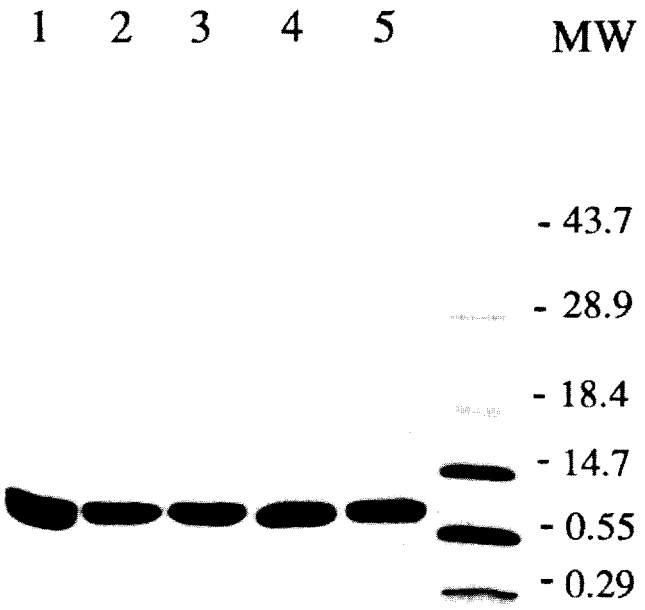

Figure 2. Electrophoresis of purified wild-type mutant EcCMs. Samples (6 μg) of each protein were loaded on a 16% SDS gel. The molecular mass markers are indicated in kD at the right. Lane 1: Lys39Arg; lane 2: Lys39Asn; lane 3: Lys39Gln; lane 4: Gln88Glu; lane 5: wild-type EcCM.

weaker. The data confirm that no major conformational changes result from the point mutations.

Activity and kinetic analyzes

The specific activity of each purified protein, determined by monitoring the conversion of chorismate to prephenate at 37 °C in 50 mM Tris (pH 7.8), is shown in Table 1. Since NK6024 has the *pheA*$^-$ tyrA$^+$ genotype, it was especially important to rule out any contaminating mutase activity from small quantities of the bifunctional *E. coli* T-protein (chorismate mutase/prephenate dehydrogenase) on the tyrosine biosynthetic pathway. Therefore, each EcCM mutant enzyme was assayed both for prephenate dehydrogenase and

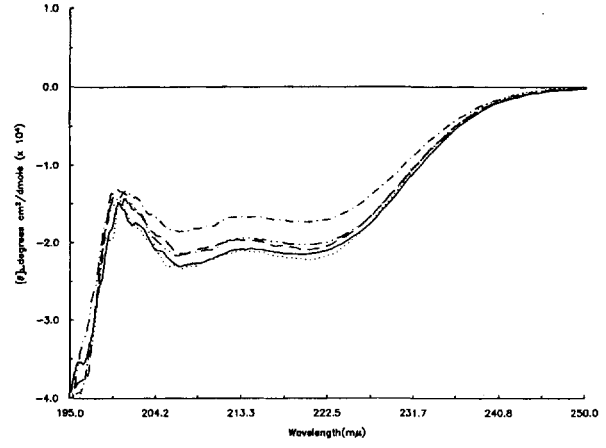

Figure 3. Circular dichroism spectra of wild-type and mutant EcCMs are presented as mean residual ellipticity. Wild-type (———), K39R (·····), K39N (– – – –), K39Q (–·–·–), and Q88E (–··–··–).

Table 1. Specific activity of wild-type and mutant EcCM

Clone	Mutant	Specific activity (units/mg)[a]	Specific activity (mutant) / Specific Activity (WT)
pJS47	wild-type	124 ± 19[b]	1.0
pSZ27	Lys39Arg	0.27 ± 0.06	2.2×10^{-3}
pSZ28	Lys39Asn	0.132 ± 0.002	1.1×10^{-3}
pSZ29	Lys39Gln	0.02 ± 0.0004	1.6×10^{-4}
pSZ30	Gln88Glu	1.25 ± 0.06	1×10^{-2}
pSZ30	Gln88Glu	243 ± 20 (pH 4.5)	1.4 (pH 4.5)
pSZ31	Gln88Arg	[c]	[c]

[a] One unit of enzyme converts 1 μmol of substrate to product in 1 min under the assay conditions (see Experimental section).
[b] Values represent the mean standard deviation of three to five measurements.
[c] Not expressed in *E. coli*.

prephenate dehydratase activity using 5–20 times the usual quantity of protein. No detectable levels of either enzymatic activity was observed. These controls confirmed the mutase activity of Lys39Arg and Gln88Glu mutants, and further established the effectiveness of the ACA54 gel-filtration column in mutant purification. Values of K_m and V_{max} for each protein were then determined by fitting initial rate data to the Michaelis–Menten equation and are shown in Table 2.

The 113-residue EcCM displayed a specific activity of 124 ± 19 units/mg. The K_m for chorismate was 290 μM, and the K_i for inhibitor **3** was 2 μM.[9] As seen in Table 2, the K_{cat} values for Lys39Arg, Lys39Asn, and Lys39Gln were 335-, 820-, and 4090-fold lower than wild-type EcCM. The residual catalytic turnover by the Lys39Arg mutant, as judged by the 335-fold drop in K_{cat}, is significant, and suggests that arginine may substitute for lysine as a positively charged and/or H-bonding residue in the catalytic mechanism. The somewhat longer side chain and branched guanidine functional group of Arg39 may distort its interaction with O7 of the inhibitor as well as with other active residues. Steric congestion might also affect the integrity of the charged network or disrupt the extensive H-bonding network.

Replacing Lys39 with asparagine or glutamine retained the H-bonding capability of the wild type residue, albeit in shortened amide side chains, but further diminished kcat, as would be expected in eliminating a key electrostatic interaction with the C11 carboxylate group. There were no significant differences in K_m or K_i between Lys39Arg, Lys39Asn, and wild-type, suggesting that Lys39 may be more directly involved in catalysis rather than substrate binding.

The Gln88Glu mutant possessed the highest activity of all mutant proteins examined, displaying 1% of wild-type activity at pH 7.8. The value of K_{cat}/K_m for Gln88Glu was also the closest to native enzyme, displaying a 445-fold reduction compared to wild-type EcCM at pH 7.8. Moreover, the higher K_m value of the

Table 2. Kinetic parameters of WT and mutant EcCM at pH 7.8

	WT	Lys39Arg	Lys39Asn	Lys39Gln	Gln88Glu
K_{cat} (min^{-1})[a]	2482 ± 287[b]	7.4 ± 0.66	2.95 ± 0.05	0.59 ± 0.01	[c]
K_m (mM)	0.30 ± 0.01	0.59 ± 0.05	0.45 ± 0.03	1.16 ± 0.08	[c]
K_{cat}/K_m ($mM^{-1}min^{-1}$)	8.24 ± 1.1 × 10^3	12.7 ± 2	6.65 ± 0.5	0.51 ± 0.03	18.5 ± 0.4
K_i (μM)	3.21 ± 0.22	3.69 ± 0.64	7.32 ± 1.0	7.52 ± 1.5	[c]
K_{cat} (mutant) / K_{cat} (WT)	1.0	3×10^{-3}	1.2×10^{-3}	2.4×10^{-4}	[c]
K_{cat}/K_m (mutant) / K_{cat}/K_m (WT)	1.0	1.5×10^{-3}	8.1×10^{-4}	6.2×10^{-5}	2.3×10^{-3}

[a]Because of excessive UV absorbance at high substrate concentration, the concentration of free chorismate was limited to 3 mM in kinetic assays.
[b]Values represent the mean standard deviation of three measurements.
[c]In the case of Q88E, saturation was not observed even at 3.33 mM substrate. As a result, K_{cat}, K_m and K_i values could not be determined; however, K_{cat}/K_m was determined by a linear fit of initial velocity vs low substrate concentration ($v = S\,V_{max}/K_m$) at less than 0.2 mM chorismate.

Gln88Glu mutant at pH 7.8 also suggested that Gln88 may also play a role in substrate binding through hydrogen bonding interactions with O7.

The activity of the Gln88Glu mutant was found to be highly pH-dependent, rising dramatically under acidic conditions. At its optimum pH (4.5), the Gln88Glu mutant displayed 140% of wild-type EcCM activity (Table 1), largely because of enhancements in turnover ($k_{cat} = 9700\ min^{-1}$ for the mutant; $k_{cat} = 3700\ min^{-1}$ for wt, both at pH 4.5). This finding was especially interesting in view of computer simulations on ScCM, both by us at Cornell[17] and by Xue and Lipscomb at Harvard.[7] Molecular modelling of the solid state structure of uncomplexed ScCM with the structure of the EcCM • **3** complex (Fig. 4) indicated that a glutamic acid residue in ScCM (Glu 246) replaced the Gln88 of EcCM. The change from Gln to Glu in ScCM also significantly lowered its pH optimum,[18] as would be expected in order for Glu to function as a hydrogen bond donor.[9]

The structure of the Gln88Glu mutant mutase was further probed in an energy minimization study using the crystallographic coordinates of the wild-type EcCM • **3** complex as a reference (see Fig. 5). Given the minimal change in residue size, relatively little perturbation was observed in the mutant, although glutamate at position 88 was noticeably displaced from the bound inhibitor. Specifically, the interatomic distance between O7 of **3** and the amide NH of Gln88 (2.88 Å in wild type EcCM) increased to a distance of 3.53 Å between O7 of **3** and the corresponding carboxylate oxygen of Glu88 in the final model of the mutant. As a result, two hydrogen bonds involving Gln88 of wild-type EcCM (one to inhibitor **3** and one to Ser84) were forfeited in the Gln88Glu mutant. However, the positional shift of Glu88 compensated for this loss with two new hydrogen bonds to the terminal NH of Lys39 and to the main chain NH of Gly36 (not shown) at distances of 2.73 and 3.10 Å, respectively (Fig. 5).

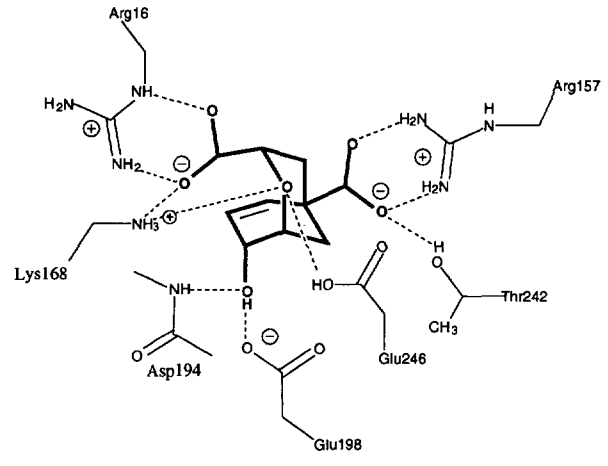

Figure 4. Schematic diagram indicating the hydrogen bonds and electrostatic interactions of transition state analogue inhibitor **3** with relevant side chains of ScCM, as determined from molecular modelling by comparing the X-ray structure of uncomplexed ScCM with that of the EcCM • **3** complex.

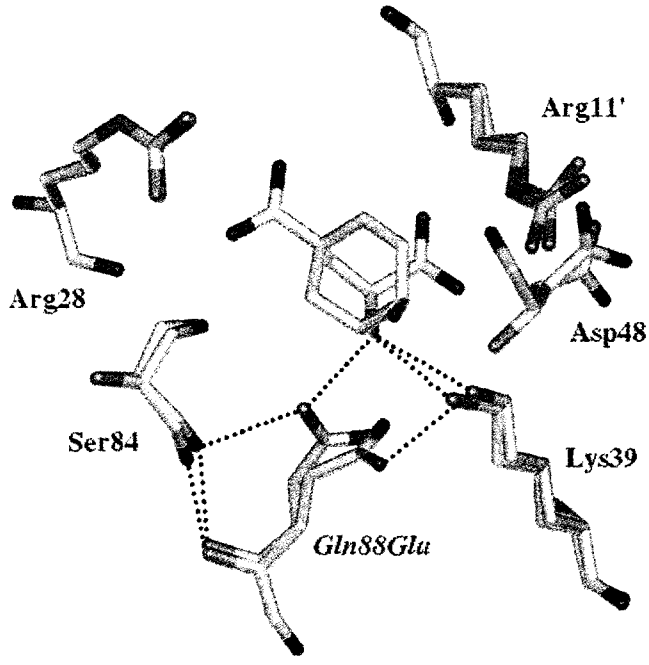

Figure 5. Structural changes resulting from the replacement of Gln88 with Glu in EcCM as reflected by molecular modelling and energy minimization studies. Lines indicate selected hydrogen bonds formed with Lys39, Ser84, and the residue at position 88. The figure also indicates slight shifts in the positions of surrounding residues Arg11′, Arg28, Lys39, Asp48, and Ser84. In the interest of clarity, only one molecule of inhibitor **3** is shown.

Conclusion

We have proposed that EcCM, BsCM, and ScCM function by a common mechanism whereby (1) adjacent, protonated, active-site residues exert conformational control in the chorismate mutase E–S complex, and (2) hydrogen bonding between active-site residues and O7 of bound chorismate further catalyzes the rearrangement. Besides rationalizing all available experimental data on the chorismate mutase reaction, these mechanistic ideas are further supported by the mutagenesis studies reported herein.

The significant variations in active-site structures of EcCM, BsCM, and ScCM suggest that nature has evolved a variety of catalytically active motifs by which the rearrangement of **1** can be accelerated. Clearly, additional mutagenesis studies are needed to test other active-site residues in order to gain more complete insight into the detailed mechanism of chorismate mutase.[19]

Experimental

Strains, plasmids and growth of organism

Escherichia coli NK6024 (relevant genotype: *pheA*$^-$ *tyrA*$^+$) was used as the host for cloning, plasmid isolation, and expression.[20] Plasmid pJS47 encoding the 113 residue EcCM was constructed from pJS42[21] as follows. Digestion of pJS42 with *AfI* II and *Stu* I, followed by filling in the recessed *AfI* II ends and blunt-end ligation, gave pJS44. This treatment removed 106 bp of the *pheA* attenuator located 49 bp upstream of the P-protein start codon. Insertion of a 500 bp *Eco*RI filled-terminator from pKK62b-7 at the filled-in *Hind*III site of pJS44 afforded pJS47.[22] Using pJS47 as a template for generating mutations by PCR, the plasmids pSZ27 to pSZ31 were constructed as described below. Unless indicated, all strains harboring plasmids were grown in either M9 medium, Luria broth, or LB plates containing 100 μg/mL of ampicillin.

Mutagenesis and recombinant DNA manipulations

All mutations were generated by the PCR overlapping extension method.[14] Two complementary mutagenic oligonucleotides (25–31mers) were synthesized by the Cornell Biotechnology Facility and used for each mutant. All primers contained a unique restriction enzyme site without altering the amino acid coding sequence. The first round of PCR was carried out at 95 °C for 1 min, 55 °C for 1 min and 72 °C for 1 min with 35 cycles. The second round of PCR was performed at 95 °C for 1 min, 69 °C for 1 min and 72 °C for 1 min in the first 10 cycles followed by 35 cycles at 95 °C for 1 min, 55 °C for 1 min and 72 °C for 1.5 min. The resulting PCR products and pJS47 were cut with *Eco*RI and *Xba* I, and the desired DNA fragments were isolated on an 0.9% agarose gel, ligated, and transformed into NK6024 by the TSS method.[23] The resulting transformants were screened by restriction site analysis to identify positive plasmids which were called pSZ27 to pSZ31, respectively, for the five mutants (Table 1). Plasmids pSZ27 to pSZ31 containing the mutant gene and its promoter were further sequenced on an ABI Model 373A DNA Sequencer by the Cornell Biotechnology Facility.

Overexpression and purification of the wild-type and mutants

To test whether the mutants were expressed in the host cells, crude cell extracts made from each mutant and from wild-type cells were screened by Western blotting.[24] The proteins were separated by 16% SDS–PAGE, electrophoretically transferred to a nitrocellulose membrane, and probed with rabbit anti-P protein antibody followed by reaction with goat anti-rabbit antibody linked to alkaline phosphatase. Finally the EcCM bands were visualized with NBT and BCIP.

EcCM was purified by the published procedure[21] with several modifications. Freshly transformed colonies containing the desired plasmid were inoculated into 40 mL of LB culture and grown with rotary shaking at 37 °C until the OD_{600nm} reached 1.0. The LB culture was used to inoculate 2 L of M9 medium supplemented with 7.0 μg/mL of phenylalanine, 230 μg/mL of proline, 17 μg/mL of thiamine, and 0.8% of glucose (mutase expression was found to be 3–6 times higher in M9 compared to LB). After growth at 37 °C for about 4–5 h (OD_{600nm} around 0.5) the culture was induced with 0.5 mM IPTG and allowed to grow overnight. Cells were harvested by centrifugation, the pellet was resuspended in 20 mL of 100 mM Tris (pH 8.5), 5 mM EDTA and 1 mM PMSF and french pressed at 10 000 lb/in^2. The extract was centrifuged at 14000 rpm for 30 min and 0.15 volume of 30% streptomycin sulfate was added to the supernatant. After centrifugation, the supernatant was adjusted to 2.3 M with $(NH_4)_2SO_4$ and allowed to precipitate on ice for 30 min. The precipitate was collected by centrifugation and dissolved in 20 mM Tris (pH 8.5) plus 10% glycerol and dialyzed against the same buffer. The dialyzed sample was loaded on a Q-Sepharose column (2×10 cm) equilibrated previously with 20 mM Tris pH 8.8, 10% glycerol, and eluted with a linear gradient (2×300 mL) of 0–100 mM NaCl in equilibration buffer. Active fractions were concentrated to about 10 mL on an Amicon filter and further chromatographed on a 500 mL Ultrogel ACA54 column (2.6×100 cm) using 50 mM Tris, 100 mM NaCl, 10% glycerol as elution buffer (pH 8.2). Protein purity was assessed on a 16% SDS-gel. Protein concentration was measured by the Bradford assay using BSA as the standard.[25]

Kinetic characterization

For each mutant, chorismate mutase activity was measured as previously described[26] at 37 °C for 5 min in 50 mM Tris (pH 7.8, except as noted), 2.5 mM EDTA, 20 mM mercaptoethanol and 0.01% BSA with 1 mM chorismic acid. Values of K_i for **3** with each

mutant were determined at a final inhibitor concentration (3–12 μM) and varying substrate concentrations (100 μM, 2 mM) using Lineweaver–Burk plots, fitting the data to the standard model for competitive inhibition using the equation $K_{m\,(apparent)} = K_m\,(1 + I/K_i)$.

Circular dichroism analysis

CD spectra were determined on a modified Cary Model 14 at room temperature following a general protocol.[27] Temperature was maintained at ±0.1 °C with a Polyscience Model 9110 circulating bath. CD spectra were obtained at a protein concentration of 30 μg/mL in 50 mM potassium phosphate buffer (pH 7.0) using a 1 cm path length cell. Spectra were recorded 2–4 times for each sample from 290 to 190 nm at a scanning rate of 0.5 Å/s. Data were digitized with an integration time of 1 s and stored on a SUN IPC computer.

Energy minimization studies

Energy minimizations using the Adopted-Basis Newton Raphson (ABNR) protocol were performed employing CHARMm in QUANTA, distributed by Molecular Simulations Incorporated. Calculations were performed within a radius of 10 Å from the carboxylate oxygen of Glu88, having the bound inhibitor **3** present in the model at all times. Hydrogen bonded and nonbonded lists of the molecule were created prior to the energy evaluation and subsequent minimization by QUANTA.

In the first step, the modified sidechain was allowed to move, and the energy minimization was performed until the root mean square gradient was lower than 0.01 kcal/Å. In the next step, all side chains of the active-site residues were allowed to move with their backbone atoms constrained. In the final step, the backbone atoms of the active-site residues were included for energy minimization. In each step, energy minimizations were carried out until the root mean square gradient was lower than 0.01 kcal/Å.

Acknowledgements

Financial support by grants from the National Institutes of Health to BG (NIH GM 24054) and JC (NIH CA 24487) are gratefully acknowledged. We also thank Mr Gary Davenport for assistance in obtaining CD spectra.

References

1. Haslam, E. *Shikimic Acid Metabolism and Metabolites*; John Wiley: New York, 1993.

2. Andrews, P. R.; Smith, G. D.; Young, I. G. *Biochemistry* **1973**, *18*, 3492.

3. Gorisch, H. *Biochemistry* **1978**, *17*, 3700.

4. Bartlett, P. A.; Johnson, C. R. *J. Am. Chem. Soc.* **1985**, *107*, 7792.

5. Lee, A. Y.; Karplus, P. A.; Ganem, B.; Clardy, J. *J. Am. Chem. Soc.* **1995**, *117*, 3627.

6. Chook, Y.-M.; Gray, J. V.; Ke, H.; Lipscomb, W. N. *J. Mol. Biol.* **1994**, *240*, 476.

7. Xue, Y.; Lipscomb, W. N. *Proc. Natl. Acad. Sci. U.S.A.* **1995**, *92*, 10595.

8. Haynes, M. R.; Stura, E. A.; Hilvert, D.; Wilson, I. A. *Science* **1994**, *263*, 646.

9. Lee, A. Y.; Clardy, J.; Stewart, J. D.; Ganem, B. *Chem. Biol.* **1995**, *2*, 195.

10. Coates, R. M.; Rogers, B. D.; Hobbs, S. J.; Peck, D. R.; Curran, D. P. *J. Am. Chem. Soc.* **1987**, *109*, 1160.

11. Gajewski, J. J.; Jurayj, J.; Kimbrough, D. R.; Gande, M. E.; Ganem, B.; Carpenter, B. K. *J. Am. Chem. Soc.* **1987**, *109*, 1170.

12. Severance, D. L.; Jorgensen, W. L. *J. Am. Chem. Soc.* **1992**, *114*, 10966.

13. Curran, D. P.; Kuo, L. H. *Tetrahedron Lett.* **1995**, *36*, 6647.

14. Ho, S. N.; Hunt, H. D.; Horton, R. M.; Pullen, J. K.; Pease, L. R. *Gene* **1989**, *77*, 51.

15. Stewart, J. D.; Wilson, D. B.; Ganem, B. *Tetrahedron* **1991**, *47*, 2573.

16. Yang, J. T.; Wu, C. S. C.; Martinez, H. M. *Methods Enzymol.* **1986**, *130*, 208.

17. Kongsaeree, P.; Clardy, J. C. *Abstracts of the Annual Meeting of the American Crystallographic Association,* Montreal, Quebec, Canada, 23–28 July, 1995.

18. Schmidheini, T.; Mösch, H.-U.; Evans, J. N. S.; Braus, G. *Biochemistry* **1990**, *29*, 3660.

19. While this manuscript was under review, related studies on EcCM and BsCM appeared in print: (a) Cload, S. T.; Liu, D. R.; Pastor, R. M.; Schultz, P. G. *J. Am. Chem. Soc.* **1996**, *118*, 1787; (b) Liu, D. R.; Cload, S. T.; Pastor, R. M.; Schultz, P. G. *J. Am. Chem. Soc.* **1996**, *118*, 1789.

20. We are grateful to Dr N. Kleckner of Harvard University for providing this strain.

21. Stewart, J. D., Ph.D. Thesis, Cornell University, 1991. Copies available upon request.

22. Brosius, J. *Gene* **1984**, *27*, 161.

23. Chung, C. T.; Niemela, S. L.; Miller, R. H. *Proc. Natl. Acad. Sci. U.S.A.* **1989**, *86*, 2172.

24. Towbin, H.; Staehelin, T.; Gordon, J. *Proc. Natl. Acad. Sci. U.S.A.* **1979**, *76*, 4350.

25. Bradford, M. M. *Anal. Biochem.* **1976**, *72*, 248.

26. Gething, M. H.; Davidson, B. E.; Dopheide, T. A. A. *Eur. J. Biochem.* **1976**, *71*, 317.

27. Adler, M.; Scheraga, H. A. *Biochemistry* **1988**, *27*, 2471.

(*Received in U.S.A.* 31 *January* 1996; *accepted* 14 *March* 1996)